

Article

Steps towards Modeling Community Resilience under Climate Change: Hazard Model Development

Kendra M. Dresback ^{1,*}, Christine M. Szpilka ¹, Xianwu Xue ², Humberto Vergara ³,
Naiyu Wang ⁴, Randall L. Kolar ¹, Jia Xu ⁵ and Kevin M. Geoghegan ⁶

¹ School of Civil Engineering and Environmental Science, University of Oklahoma, Norman, OK 73019, USA

² Environmental Modeling Center, National Centers for Environmental Prediction/National Oceanic and Atmospheric Administration, College Park, MD 20740, USA

³ Cooperative Institute of Mesoscale Meteorology, University of Oklahoma/National Weather Center, Norman, OK 73019, USA

⁴ College of Civil Engineering and Architecture, Zhejiang University, Hangzhou 310058, China

⁵ School of Civil and Hydraulic Engineering, Dalian University of Technology, Dalian 116024, China

⁶ Northwest Hydraulic Consultants, Seattle, WA 98168, USA

* Correspondence: dresback@ou.edu; Tel.: +1-405-325-8529

Received: 30 May 2019; Accepted: 11 July 2019; Published: 16 July 2019



Abstract: With a growing population (over 40%) living in coastal counties within the U.S., there is an increasing risk that coastal communities will be significantly impacted by riverine/coastal flooding and high winds associated with tropical cyclones. Climate change could exacerbate these risks; thus, it would be prudent for coastal communities to plan for resilience in the face of these uncertainties. In order to address all of these risks, a coupled physics-based modeling system has been developed that simulates total water levels. This system uses parametric models for both rainfall and wind, which only require essential information (e.g., track and central pressure) generated by a hurricane model. The system is validated with Hurricane Isabel hindcasts: One using the parametric system and another using data assimilated fields. The results show a good agreement to the available data, indicating that the system is able to adequately capture the hazards using parametric models, as compared to optimized fields. The validated system was then utilized to simulate randomly generated scenarios that account for future uncertainty, i.e., amount of sea level rise and storm strength/track, as influenced by projected climate change scenarios. Results are then used in next step in the development of a system-wide, community resilience model.

Keywords: total water level; tropical cyclones; climate change; coastal resilience; coupled model system

1. Background and Motivation

The hurricane seasons of 2017 and 2018 proved to be devastating for many in and around the coastal communities within the United States and island nations in the Caribbean. This devastation shows the need for improving the coastal resilience of buildings and civil infrastructure that are needed in order to protect many of the city and county services following a natural disaster.

With Hurricane Harvey during the 2017 season, the damage associated with the storm was caused by wind and flooding from both storm surge and rainfall. Blake and Zelinsky [1] indicated in their NOAA report that the estimated damage from the storm was \$125 billion, which falls near the estimates for Hurricane Katrina. Southeastern Texas received a significant amount of the damages: Over 300,000 structures were flooded and over 336,000 customers lost their power from the hurricane [1]. Harvey had an extraordinary amount of rainfall associated with the storm over the coastal regions of Texas

with the Houston area experiencing approximately 36 to 48 inches total during the storm. As well, some of the cities along the Texas/Louisiana border received over 60 inches. All of the rain caused many of the rivers within the Houston metro areas to exceed their banks and lead to record flood stages on Clear Creek, Dickinson Bayou, Buffalo Bayou and Cypress Creek [1].

Hurricane Irma followed Hurricane Harvey by a couple of weeks and made landfall in Florida. Similar to Harvey, Irma produced damages that were caused by wind and flooding due to both storm surge and rainfall. Irma affected the Florida Keys most significantly with almost 25% of the buildings on the Keys destroyed during the storm and almost 90% of the structures sustaining damage [2]. Throughout several counties of Florida, Irma destroyed structures and caused significant power failures. Furthermore, the storm had a devastating effect on the agricultural crops, e.g., it was estimated that approximately \$760 million in damage was done to the orange groves in the southwestern and central parts of Florida [2]. Heavy rainfall occurred as Irma moved into the northern portions of Florida leading to significant flooding with rivers reaching, and some exceeding, previously recorded flood stages in nine different counties: Bradford, Clay, Marion, Flagler, Duval, Putnam, St. Johns, Nassau and Alachua [2].

Hurricane Maria was the most devastating hurricane to make landfall on any of the Caribbean islands in almost 80 years. Reports from the island nation of Dominica indicated that a majority of the structures on the island were either seriously damaged or destroyed as a result of the storm. In fact, Pasch et al. [3] indicated that the Prime Minister “described the damage as mind-boggling”. Maria caused approximately \$1.31 billion in damages in Dominica [3]. Portions of the U.S. Virgin Islands were severely affected by Maria with St. Croix experiencing some of the most extensive damage. Not only was the wind damage significant over the island nation, but also there was excessive rainfall that caused landslides and flooding [3]. The devastation caused by Hurricane Maria in both Puerto Rico and the U.S. Virgin Islands has been estimated to be approximately \$90 billion, due to both winds and flooding. Pasch et al. [3] indicates that almost 80% of the electrical grid was impacted by Maria, along with the loss of the cell service and the municipal water supply over most of the island. Hurricane Maria has been estimated as the third costliest hurricane in U.S. history, behind Hurricane Katrina and Harvey [3].

The civil infrastructure destruction that occurred during Hurricanes Harvey, Irma and Maria shows the need for improving the manner in which we manage the risk to civil infrastructure due to natural hazards. With over 40% of the population living in the coastal counties within the U.S., [4] and with that population expected to rise, there is an increasing risk that coastal communities will be significantly impacted by flooding, storm surges and high winds associated with hurricanes and tropical storms. Furthermore, climate change will exacerbate these risks in the coastal communities [5]. The current hazard modeling approaches used to manage civil infrastructure risk in the face of extreme flooding and winds are traditionally statistically-based in their evaluation [6]. To provide an example of this, one just needs to look at the Flood Insurance Rate Maps (FIRMs) developed by the Federal Emergency Management Agency (FEMA). In these maps, they depict the 100-year and 500-year return period flood contours; however, these maps do not reflect the spatial variation of the hazard demand parameters within a community, or the spatial and temporal correlations among these demands, imposed by specific flood scenarios. Such information however is critical to characterize the correct spatial distribution of risk that is paramount for natural hazard mitigation of civil infrastructure within communities. Furthermore, the concept of a “return period” implies that the extreme hazard of interest can be modeled as a stationary random process, which becomes untenable when non-stationary effects of global climate change are considered. Thus, herein and in the companion paper, we present a physics-based hazard modeling approach to evaluate risk-based coastal community resilience planning. This methodology provides an effective way of evaluating the risk and also provides time series of hazard demand parameters (i.e., water depth, flood duration, flow velocity, etc.) to support resilience assessment at community or regional scales. Additionally, this methodology provides a way to capture the impact of climate change (non-stationarity) on hazard intensity and frequency of occurrence.

Others have looked at community resilience and the coastal flooding [7–11] for Hurricane Sandy and other storms; however, in many of these studies they look at only the storm surge and wave influences in the coastal flooding. In particular, Lin et al. [11] analyzed the coastal flooding caused by Hurricane Sandy and what impacts climate change would have had on the coastal flooding of the storm. Hatzikyriakou and Lin [9] looked at a vulnerability analysis for the coastal flooding that occurred during Hurricane Sandy for the coastlines of New York and New Jersey. However, Wahl et al. [12] indicated that there should be a consideration of the compound flooding that occurs due to the rainfall-runoff effect and its connection to the coastal flooding. In their work, they indicated that the compound effects of both storm surge and rainfall-runoff occurring are greater than each of the phenomena separately. Additionally, they found that the likelihood of the joint occurrence of these were greater in the Atlantic and Gulf Coast states than those of the Pacific Coast state [12]. Furthermore, they also found that there seems to be an increase in these compound events occurring over the past 100 years. The examples of the hurricanes given above show that the compound flooding can cause significant damage. Recent studies by several researchers [13–16] have shown the impacts of rainfall-runoff on coastal flooding. Furthermore, Yang et al. [17] demonstrated the significant impact combined flooding can have on the timing and spatial location of evacuation orders given during hurricane events.

In this manuscript, we will present a physics-based, coupled model system that provides the inundation and wind hazards for use in coastal resilience risk management. In particular, we will utilize this system to evaluate tropical cyclone storms that incorporate climate change and develop inundation scenarios that can be utilized by the risk management model. The layout of the paper is as follows: Section 2 discusses the development of this expanded coupled modeling system, which is called STORM-CoRe [18]; Section 3 discusses the validation of this coupled modeling system using Hurricane Isabel as a test case; Section 4 discusses the methodologies used in the evaluation of future storms that include climate change; Section 5 discusses some of the results that are used for the infrastructure resilience assessment. In Section 3, we use Hurricane Isabel as a case study, which has been utilized to evaluate several other coupled modeling systems [14,19]. Isabel occurred in September 2003 and made landfall as a Category 2 storm in North Carolina near Drum Inlet on September 18th at 1700 UTC (Coordinated Universal Time). The storm weakened after making landfall and dissipated over western Pennsylvania by 19 September. Isabel created storm surges of 1.8–2.4 m along the coast of North Carolina and 1.2–1.8 m along the coast of Virginia; winds at Cape Hatteras, North Carolina were recorded at 70 knots with gusts at 88 knots [20]. Hurricane Isabel produced 10–18 cm of rainfall over eastern North Carolina, with 20–30 cm occurring in the Virginia area. Isabel resulted in one direct and two indirect casualties within the North Carolina area [20], and damages for the same area were estimated to be \$170 million.

2. Materials and Methods

There are several flood modeling approaches that have been developed in the past 15 years that use coupled models to forecast flood extents or provide guidance to emergency managers in the case of tropical storms or hurricanes [13,21–23] and provide guidance for water quality issues [24,25]. A logical next step is to couple these advanced hazard modeling techniques to civil infrastructure risk management models in order to enhance community resilience in the face of tropical storms and hurricanes. One such effort has led to the development of a coupled modeling system, called STORM (Scalable, Terrestrial, Ocean, River, Meteorology [13]), which couples hurricane wind and precipitation, hydrologic, wave and hydrodynamic models to predict total water levels (tides + waves + surge + runoff) due to tropical storms and hurricanes. Herein, the research builds on the STORM system with a novel approach to provide hazard impacts for coastal communities based on possible future events. The new coupled modeling system will be denoted STORM-CoRe (Coastal Resilience) [18] because the results from the system will be utilized to support coastal resilience planning under climate change. The coupled model system is applicable to any geographic region, with the caveat that each of

the individual model components must be developed for a specific domain. Figure 1 illustrates the STORM-CoRe system and the data that are shared between the models, along with the model results that are passed on to the community resilience planning process. In the subsections below, each of the models utilized in the STORM-CoRe system are described; with the exception of the Infrastructure Resilience Assessment model development, which is the subject of a related paper [26].

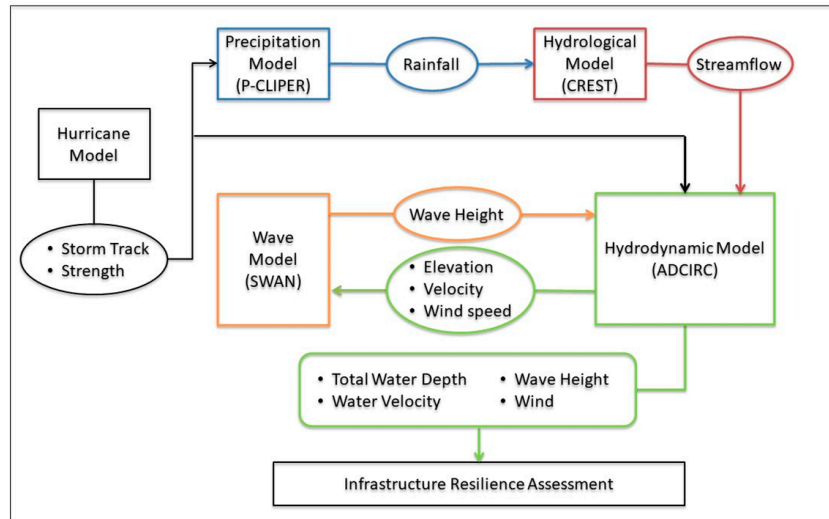


Figure 1. Schematic of the STORM-CoRe coupled modeling system: Models are shown in boxes, model output in ovals, and arrows indicate the information that is passed to each model as input. All information that is passed to the Infrastructure Resilience Assessment modeling team passes through the ADCIRC model and is denoted by the rounded rectangle.

2.1. Hurricane Model

The model utilized to develop the hurricane tracks, strengths and wind fields for the synthetic tropical storms was developed by Emanuel et al. [27–30]; it is a global, physics-based model that has the ability to capture the impact of climate change on the formation of hurricanes and tropical storms. This model produces wind fields for hurricanes and tropical storms through the development of an operating vortex that is able to interact with atmospheric winds and interface with the sea surface water. These winds can then be utilized with a global circulation model or global forecast system in the development of hurricanes and tropical storms that take into account climate change. In contrast, statistically-based hurricane models typically used to develop tracks and intensities are not capable of systematically incorporating future trends, thus making it hard to include climate change in the development of hurricanes and tropical storms used to determine the impacts and risks to civil infrastructure [31]. Several recent studies [29,32,33] have shown that the inclusion of climate change in assessing the risk of civil infrastructure due to tropical storms and hurricanes in the future is necessary due to the trends that have been seen in the frequency and intensity of extreme storms. Due to the global nature of the model, it is easy to select storms that make landfall in any particular study area.

2.2. Synthetic Parametric Tropical Cyclone Rainfall Model, P-CLIPER

In order to predict the rainfall rates needed to drive the hydrological model, STORM-CoRe utilizes a newly-developed synthetic parametric tropical cyclone rainfall model, called PDF Precipitation-Climatology and Persistence (P-CLIPER) [34]. The probability density functions (PDFs) utilized in P-CLIPER are developed from the precipitation information collected from the satellite-based Tropical Precipitation Monitoring Mission (TRMM) over a three-year period, which had over 2121 precipitation events recorded. The parametric equations developed from this information can be found in Geoghegan et al. [34]. There are three intensity categories utilized in the model: Tropical Storm (TS), Category 1 and 2 (CAT12), and Category 3, 4, and 5 (CAT345). P-CLIPER uses the tropical

cyclone track and strength information obtained from the hurricane model discussed in the previous section to develop the rainfall intensities. More specifically, it utilizes the radius from the center of the storm, along with the departure from the average rainfall intensity as represented by a frequency parameter, f , that allows the rainfall intensities to change in the model. Negative values provide weaker rainfall intensities with less of a rainfall gradient from the center to the outer radius of the storm, while positive values provide stronger rainfall intensities with a higher rainfall gradient throughout the radius of the storm. While the radius is obtained from information developed out of the hurricane model, the frequency is independent from the hurricane model and can vary based on the strength of the storm. Geoghegan et al. [34] analyzed several storms within North Carolina to determine if there was a guideline for determining the frequency value; however, it was found that there was a range of applicable values that depended on a complex interaction of the storm's character and the landfalling region. Therefore, it is important to analyze the frequency for each individual study area before applying P-CLIPER. For this study, the frequency was randomly sampled from the range identified from the North Carolina study (more on this in Section 4.2).

2.3. Hydrology Model, CREST

The hydrology model used in the STORM-CoRe system is the Coupled Routing and Excess Storage (CREST) model [35,36]. CREST is a distributed hydrologic model that utilizes the variable infiltration capacity curve [37–40] to determine the surface runoff and infiltration in each cell. It also employs linear reservoir theory to calculate the surface and subsurface flow. This information is then routed downstream cell-by-cell using the flow direction, flow accumulation and the slope determined from the Digital Elevation Model (DEM). An automatic calibration technique, called SCE-UA (shuffled complex evolution [41,42]), can be utilized automatically to set the model parameters. Additionally, CREST has the ability to use grid-based parameters, which can be estimated a-priori from high-resolution land use/land cover maps, soil texture data, and other remotely sensed data. CREST has data assimilation schemes implemented within it that can utilize observations, such as streamflow or soil moisture. CREST has been applied throughout the world [43–45] and was recently adopted by NOAA's National Severe Storms Laboratory to provide guidance during flash flood events [46]. In STORM-CoRe, streamflows from CREST, as driven by P-CLIPER results, are used to provide the hydrologic boundary conditions to the hydrodynamic model (discussed in Section 2.5).

2.4. Wave Model, SWAN

The Simulating Waves Nearshore (SWAN) model serves as the wave model in the STORM-CoRe coupled model system. SWAN is based on the wave action balance equations; full development of the model equations can be found in Booij et al. [47]. SWAN includes the following physical processes: wave refraction and diffraction, wave frequency with the change in water depth or current, and the spatial and temporal parts of wave propagation. Furthermore, SWAN takes into consideration several parameterizations for the bottom friction, nonlinear effects due to changes from deep to shallow region, white-capping of waves and their loss of energy and the surf breaking [47]. Over the last decade, SWAN has been expanded to utilize unstructured grids [48], thus making it easier to tightly couple it to unstructured hydrodynamic models [49]. This tight coupling allows the wave and hydrodynamic models to share information during run time and to utilize the same domain and grid in their solution. The coupling intervals between the two models can vary based on convergence behavior of the SWAN model [49]. Studies undertaken in the same region for a real-time guidance system [13,19] indicate that the ideal coupling interval between the two models is 10 min. SWAN provides wave radiation stresses to the hydrodynamic model and takes as input windspeeds, water heights and velocities.

2.5. Hydrodynamic Model, ADCIRC

The Advanced Circulation (ADCIRC [50]) model serves as the hydrodynamic model in the STORM-CoRe coupled model system. ADCIRC, which has been in use for over 35 years, has seen a

wide variety of applications, which include flood inundation maps for coastal areas [51,52], modeling baroclinic driven circulation [53], real-time prediction of storm surge to provide guidance [13,21], surge and riverine flooding [14,54–56], modeling tides and wind driven circulation [57,58] and an integrated, scenario-based evacuation and sheltering system [56,59]. The ADCIRC model employs the shallow water equations in their non-linear formulation, subject to hydrostatic and Boussinesq approximations. ADCIRC uses the generalized wave continuity equation (GWCE [60]) to obtain changes in the water surface elevations and a non-conservative form of the momentum equation to obtain changes in the velocities. When tightly coupled to SWAN, the model is often referred to as ADCIRC + SWAN.

ADCIRC serves as the integrator for all of the physics-based models in the STORM-CoRe system. It utilizes the streamflow information from the CREST model, along with the wave information from the SWAN model in obtaining the elevation and velocity changes associated with the synthetic storms. In order to incorporate the wind effects, ADCIRC employs an embedded parametric Holland model [61], which utilizes the track and storm strength information from the synthetic storms developed by the hurricane model. Additionally, overland regions can be included within ADCIRC; but land elements remain inactive (or dry) until they meet a minimum water level threshold.

2.6. Modeling Process

In practice, other computational models (e.g., WRF-Hydro[®] for hydrology model [62], Steady-State Spectral Wave Model (STWAVE) for wave model [63]) could be substituted for any of the above models. However, unless otherwise noted, herein the STORM-CoRe system utilizes the models presented in the above subsections. Additionally, any storm track (e.g., from observations) and associated strength can easily be substituted in order to forecast or hindcast.

The general order of coupling is conveyed by the arrows in Figure 1; a more detailed description of the modeling process is summarized below with further details provided in Section 4. For each storm, the following steps are followed:

1. Spin up ADCIRC for 45 days with background tides and streamflows (this step can be done once for each sea level rise scenario and then used for all storms in that scenario);
2. Obtain the storm track and strength;
3. Run P-CLIPER with a randomly sampled frequency value (runs from start of storm in open ocean until end of hurricane track record but only computes precipitation for those portions of the P-CLIPER domain within 350 km of the storm);
4. Run CREST with the precipitation from P-CLIPER to determine streamflows; CREST is run in two phases: (1) for the duration of precipitation over the CREST domain, and (2) a spindown phase with zero precipitation forcing to route the water from the upland areas down to the coastal regions;
5. Run ADCIRC+SWAN using the storm track and strength, tides and riverine boundary forcing from CREST (run during the length of the storm within the ADCIRC domain) to get the total water level for the storm phase;
6. Run ADCIRC using tides and CREST riverine boundary forcing from the time the storm ends for a total of 20 days from the time the storm began in order to get the total water level for the river spindown phase (visual inspection of hydrographs for all storms indicated that the streamflows had returned to base flow by 20 days for most storms).

The wind, total water elevations/velocities, and wave heights from all of the synthetic storm simulations (storm and river spindown phases) will then be utilized to determine the Infrastructure Resilience Assessment, which is discussed in a related paper [26]. Currently, only the total water elevations are being used for the first phase of the resilience determination.

3. Validation of the STORM-CoRe System

3.1. Domain of Study and Hurricane Isabel

The study domain for this manuscript encompasses the coastal area of North Carolina, along with the inland areas of the Tar and Neuse river basins and watersheds. This area was chosen for two reasons: To build on the historic work in this area that had been done as part of a previous project [13,14,19], and because, historically, North Carolina ranks fourth overall for the most expensive damage done by hurricanes [64]. Some of the storms that have caused significant damage for the state of North Carolina are Hurricanes Hazel, Fran, Floyd and Matthew. In addition to the Tar and Neuse Rivers, previous studies of Hurricane Floyd [14] demonstrate that Contentnea and Fishing Creeks provide a significant portion of the riverine flow during the event; therefore, all four of these watersheds are included in the coupled model. Figure 2 shows the domain of interest for the global, coastal, and inland areas; the connection or “handoff” points between the hydrologic and hydrodynamic models occurs at the four locations noted in Figure 2c, which are color coded to match the results shown in subsequent figures.

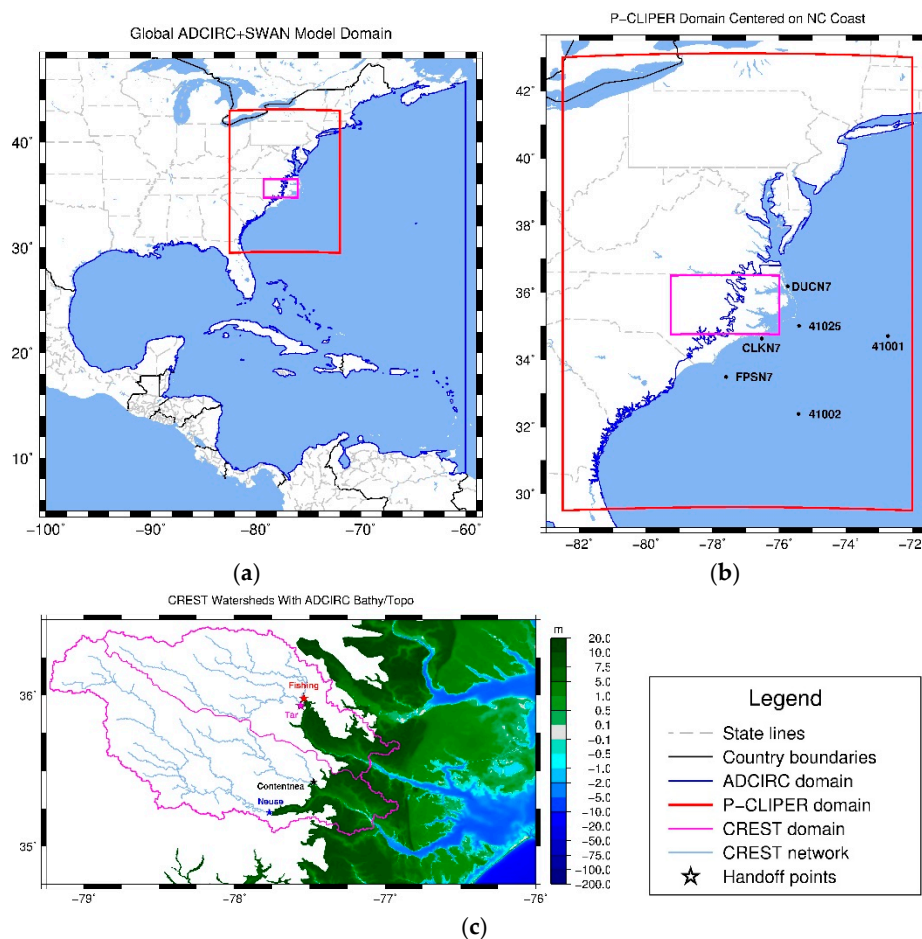


Figure 2. Study area for North Carolina coast: (a) Global ADCIRC + SWAN domain with inset boxes for other model regions; (b) P-CLIPER domain centered on North Carolina coast (location of offshore buoys used for validation in Section 3.4 shown with black dots); (c) Actual CREST domain; no stream network is shown below handoff points as this region is modeled by ADCIRC.

Herein we present a two-step validation process. In the first, we use the exact same modeling paradigm presented above in Section 2 with the exception of using the best track for Isabel instead of a synthetically derived hurricane. In the second, we use the best available data (optimized) for the wind

field, as well as measured radar precipitation instead of using P-CLIPER. For both steps, CREST and ADCIRC + SWAN are run for the same time period but with different meteorological input, see Table 1 and the following subsections for further detail. For both modeling paradigms, we compare the results of the coupled model system to high water marks collected after the storm, along with real-time gauges and buoys.

Table 1. Difference in meteorological input for two-step validation process.

Validation Step	Storm Track	Winds	Precipitation
STORM-CoRe	NOAA best track	Holland parameterized	P-CLIPER
Best Available	N/A	Data assimilated	Multi-sensor data analysis

3.2. First Step: Modeling Hurricane Isabel Using the STORM-CoRe System

In this step, we used the rainfall-runoff and wind information developed from the same models used in the STORM-CoRe system, P-CLIPER, CREST, and ADCIRC+SWAN. The best track for Hurricane Isabel is taken from the NOAA Tropical Storm report [20] and is given every 6 h from 6–19 September 2003. In order to obtain the precipitation from the P-CLIPER model, we used the calibrated value of the frequency parameter, f , and interpolated between the 6-hour intervals to provide an hourly-based track for Hurricane Isabel. Results are shown in Figure 3 (panels a, c, e and g); in future figures this simulation will be referred to as the Holland-P run because it utilizes the parametric Holland wind formulation within ADCIRC.

Notice that both the wind and precipitation are symmetric about the storm track due to the specific parametric formulations for wind and rain. Because we are running CREST in “event mode,” it did not generate streamflows at the four handoff points until 0:00 UTC on 18 September; within STORM-CoRE, ADCIRC uses a base flow of 10 cms throughout the simulation if a higher recorded value is not provided. For this storm, the coastal flooding was primarily caused by the initial storm surge; while the significant riverine flooding present in the upper reaches of the rivers was delayed by several days.

3.3. Second Step: Modeling Hurricane Isabel Using the Best Available Information

Precipitation fields were derived from a multi-sensor (radar and gauges) precipitation analyses (MPE), which were used in CREST to develop the streamflows at the handoff points. Optimized winds were developed from data assimilation techniques, which include the Interactive Objective Kinematic Analysis system (IOKA [65,66]) and the NOAA Hurricane Research Division’s Wind Analysis System [67]. The same amount of simulation time was used in this evaluation of Hurricane Isabel as the prior evaluation. Figure 3 (panels b, d, f and h) below shows the results recorded during the hindcast of Hurricane Isabel using this approach; future figures will refer to this simulation as the OWI-radar run.

3.4. Results and Discussion

Although the maximum winds from the OWI-radar run are similar in magnitude to the winds from the Holland-P run, shown in Figure 3a, they remained stronger over a wider path. The observed radar precipitation is obviously not symmetric and indicates slightly higher accumulated precipitation over the eastern watersheds (Fishing and Tar), while the P-CLIPER precipitation is higher over the western watersheds (Contentnea and Neuse). This ultimately results in the Holland-P maximum elevation results exhibiting higher overland flooding in the upper riverine areas than are seen with the OWI-radar simulation, which is a natural outcome of the higher streamflows that were calculated by CREST in the Holland-P simulation.

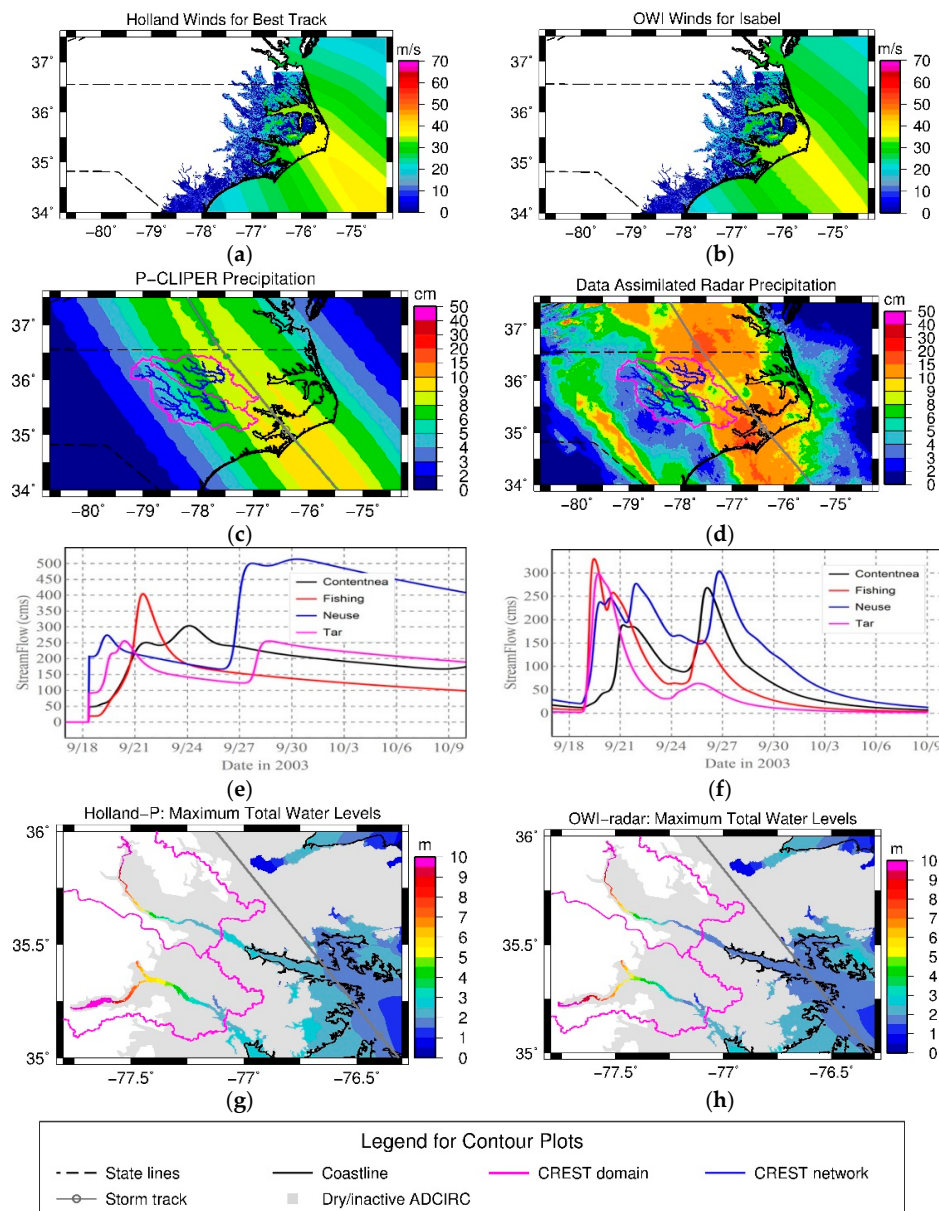


Figure 3. Results for Hurricane Isabel using the best-track within the STORM-CoRe system (panels a c e and g) and optimized wind fields and radar precipitation (panels b d f and h): (a) wind field (m/s) generated in ADCIRC with Holland model, (b) OWI wind field (m/s), CREST stream network overlaid on cumulative precipitation (cm) from (c) P-CLIPER and (d) radar, (e,f) hydrographs (cms) at four handoff points from CREST, (g,h) maximum total water elevation (m) for combined storm and river spindown in the study region.

We also observe that the prolonged streamflows in the Holland-P run (tails do not return to the base flow in Figure 3c) results in higher flooding near the coast as well; note the difference in contours between the CREST watersheds and the coastline in Figure 3g,h.

Regarding validation data for Isabel, we obtained a collection of high-water marks (HWMs) collected for the Federal Emergency Management Agency (FEMA) [68]. Additionally, during the storm, wave heights and wind speeds were recorded by National Oceanographic and Atmospheric Administration (NOAA) National Data Buoy Center (NDBC) buoys [69], and tides and surges were recorded by NOAA Center for Operational Oceanographic Products and Services (CO-OPS) stations [70]. While there are ten CO-OPS stations available in North Carolina, we focused on the four that were located in our immediate study area. Within this region, there are six NDBC buoys, four CO-OPS

stations, and 228 HWMs available. However, note that the resolution of this operational mesh is not sufficient to accurately capture surge behavior at all 228 available HWMs, therefore, only the 60 surveyed locations that have mesh resolution of less than 500 m are used herein. Figure 4 shows the locations of the various stations, buoys and HWMs used for validation (recall that the offshore buoys were shown in Figure 2b).

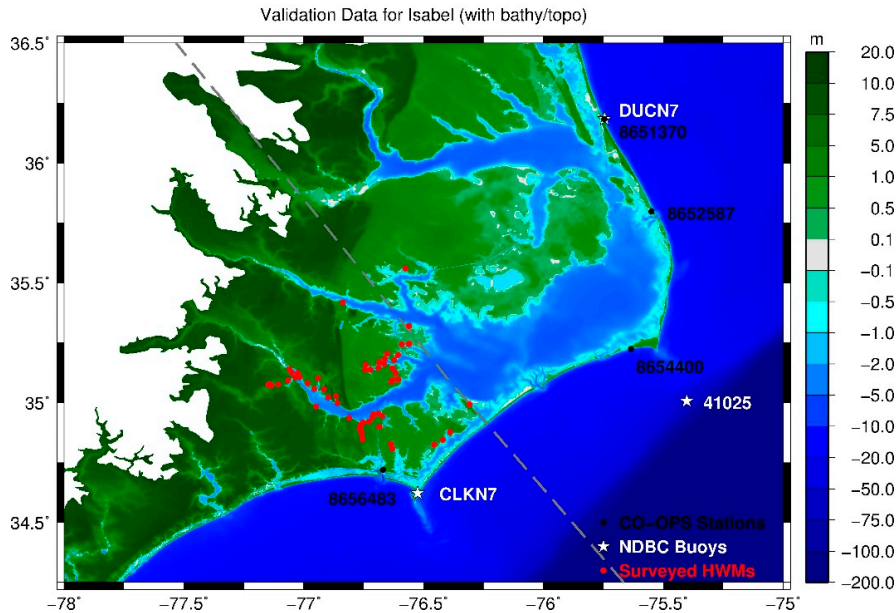


Figure 4. Location of available data used during validation of Hurricane Isabel: Dashed gray line denotes the storm track, black points denote CO-OPS stations, white stars denote NDBC buoys, and red points denote the subset of sixty HWMs which were used herein. Only the nearshore buoys are shown here, the offshore locations were given above in Figure 2b.

Time series of elevation plots at the four North Carolina CO-OPS stations are provided in Figure 5. Note that the Cape Hatteras station stopped recording during the storm, so a peak value was not available. Both models do a sufficient job of capturing the other peaks and tidal signal for all stations; however, the OWI-radar results are more accurate, which is to be expected because it uses the optimized, data-assimilated wind and precipitation data.

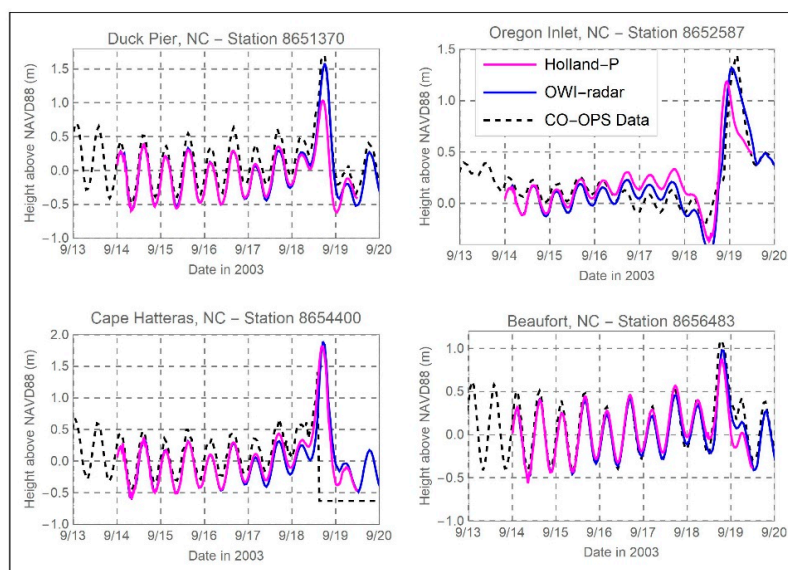


Figure 5. Elevation time series at the four North Carolina CO-OPS stations during Hurricane Isabel.

Time series of the wind speed and direction for one of the offshore and two of the nearshore buoys are shown in Figure 6. Results are not shown for nearshore buoy #41025, as it stopped recording data before the peak of the storm. Model results at both of the offshore buoys match the observed values quite well; only #41001 is shown in Figure 6. Similarly, the nearshore modelled winds match the peaks well but do not strengthen as soon in the simulation as was observed; modelled wind directions also match the observed values rather well for both nearshore and offshore locations. In general, the optimized OWI-radar simulation best captures the observed wind profiles, but both models show good fidelity to the observations.

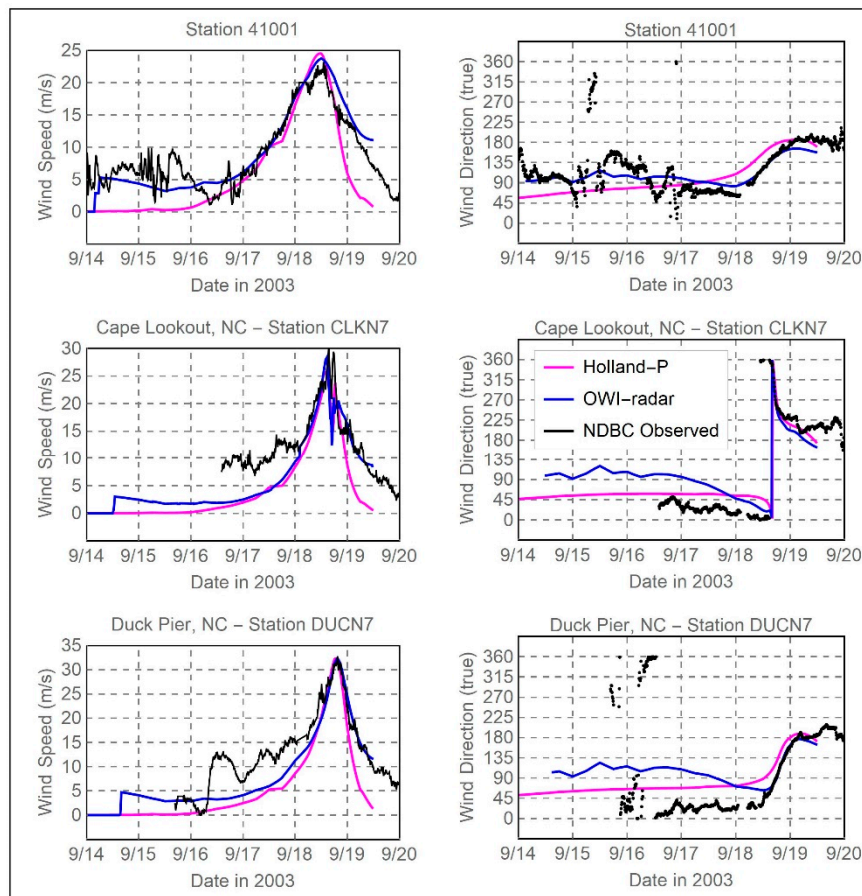


Figure 6. Wind speed and direction time series at the NDBC buoys in study area during Hurricane Isabel.

Time series for wave heights at the two offshore and one nearshore buoys are shown in Figure 7; waves are not measured at the extreme nearshore buoys (DUKN7 and CLKN7). Unfortunately, the one nearshore buoy that recorded waves (Station 41025) stopped recording data during the storm, so the peak wave height was not observed. Note that the OWI-radar simulation best captures the wave heights; however, both models capture the appropriate peaks and recessions. Additionally, it is important to note that the winds do not begin in the ADCIRC + SWAN simulations until 14 September 2003, such that both the winds and the waves take some time to ramp up in the model.

Finally, a scatter plot of modelled versus observed water heights for the 60 higher resolution HWMs and the three CO-OPS stations that recorded a peak in the North Carolina region is provided in Figure 8 (recall that Cape Hatteras (Station 8654400) stopped recording before the peak occurred). Ideally, for a perfect correlation the slope would be one and the root-mean-square error (RMSE) would be zero. Note that while the OWI-radar simulation has a lower RMSE (0.33 vs. 0.49) and the trend line is closer to an ideal slope of one (1.09 vs. 1.13), the parametric models do a reasonable job of capturing the same behavior; although there is still quite a bit of scatter in both models. The grid resolution of the

underlying ADCIRC model is optimized to provide adequate resolution to capture total water levels within the estuarine and coastal zones while still being able to simulate in a realistic timeframe (same model that is used in the real-time STORM system [13]). Furthermore, the system is not optimized for a particular storm with specific antecedent conditions and physical attributes. The results shown here are similar to results obtained in other studies with the STORM system where Hurricane Irene was analyzed with the same mesh; namely, that the best track simulation captured the HWMs with a slope of 0.90 and RMSE of 0.41 [13].

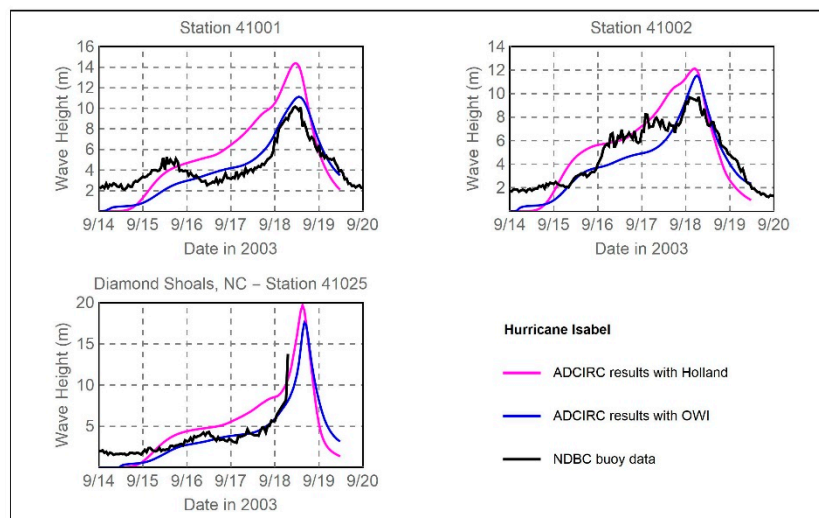


Figure 7. Wave height time series at the NDBC buoys during Hurricane Isabel.

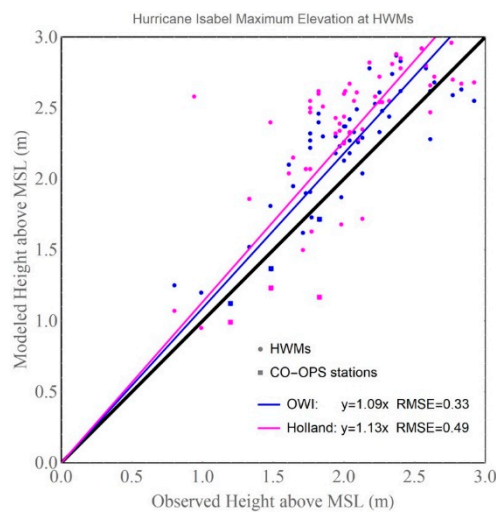


Figure 8. Scatter plot of modelled versus observed HWMs and NOS peak values.

The reader is reminded that the overall objective of this comparison is to test the predictive capabilities of the parameterized STORM-CoRe system; no attempt has been made to calibrate parameters or change grid resolution in order to more accurately capture the special features of this storm. Therefore, we are not only comparing the two model results with the observed data but also with each other in order to address this question: Is the parameterized system capable of capturing the same overall response to the hazard forcing as a simulation that uses the data assimilated observations?

As expected, the hindcast using the optimized data that was available after the storm produces smaller errors than using a parameterized wind and precipitation model (c.f. Figure 8). However, note that both the parameterized and data-assimilated wind fields in the coastal areas of North Carolina capture the overall speed and direction recorded by buoys. The precipitation between

the two methodologies shows that the parameterized rain model results in higher rainfall amounts over the western watersheds, while the Stage 4 radar products show an increase in the rainfall amounts over the eastern watersheds. These precipitation differences lead to changes in the peak streamflows. For example, in Figure 3e we see a peak for the Neuse River, which is in the western watershed, of 500 cfs with P-CLIPER input, but in Figure 3f, the peak flow for the Neuse River is 300 cfs. Furthermore, the streamflow in the Tar River is higher with the best available information due to the increase in the rainfall over the eastern watersheds (note white lines in Figure 3g,h). The increased streamflow in the Tar and Neuse Rivers make a slight difference on water levels in the coastal zone (note change from slate blue to cyan in Figure 3g,h); additionally, the increased streamflows in the Neuse River leads to changes in the upper riverine zones (note change in the magenta color between Figure 3g,h). Overall, the results indicate that use of the parametric rainfall model, P-CLIPER, in the STORM-CoRe system captures results that are similar to those using the Stage 4 observations.

Analysis of the station, buoy and HWM results show that the STORM-CoRe system produces reasonable results. Therefore, given the overall objective to use this system to study future climate scenarios, the uncertainty in the climate predictions far outweighs the model errors that result from using parametric models in lieu of observations.

4. Application of STORM-CoRe System: Stochastic Modeling for Resiliency

Having verified the model system with a historical storm, we now turn to future scenarios under climate change. The STORM-CoRe coupled model system uses a physics-based approach to generate total water levels for use in the development of a stochastic model (subject of an additional paper [26]) that will provide water levels in a given community based upon parameters from future hurricanes, subject to climate change projections. Of the many possible climate change scenarios, we utilized the “worst-case” developed by the International Panel on Climate Change [5] called Representative Concentration Pathway (RCP) 8.5 scenario. Together, RCP scenarios examine a wide range of greenhouse gas emissions that may occur in the future for years 2010–2100, with some scenarios showing a decrease in the greenhouse gas emissions over future years (i.e., RCP 2.6) to one that takes into account the increase in greenhouse gas emissions constantly through the time period (i.e., RCP 8.5) [5]. Within the coupled STORM-CoRE system, the RCP 8.5 scenario is used in the development of the synthetic tropical storms by the hurricane model and also as the initial condition in the hydrodynamic model, ADCIRC, through the sea level rise specification, which is discussed in Section 4.3.

4.1. Reduction of the Hurricane Tracks

Synthetic hurricane tracks were provided directly by Emanuel [71] from the hurricane model discussed in Section 2.1. The 5000 storm tracks that made landfall in the study area, each with its own strength, wind speed, and central pressures, were too numerous to be evaluated within the STORM-CoRe system. To reduce the number of storms, the following procedure was followed: The 5000 storm tracks were binned into 243 Latin hypercubes [72], so that each of the bins contained nearly the same number of tracks (i.e., 20 to 21 storms). Then, one of the tracks was randomly selected from each of the hypercubes, thereby reducing the number of storms to 243. In the development of the bins for the hypercube, we followed a 5-dimensional binning process that was based on the following parameters at landfall: Longitude, landing angle, pressure deficit, radius of maximum wind, and translational speed. Correlations among these parameters and the binning order might cause unexpected biases, so the sampling was run many times using different orders. Figure 9 shows the distributions of the storm strengths in this reduced set of 243 storms.

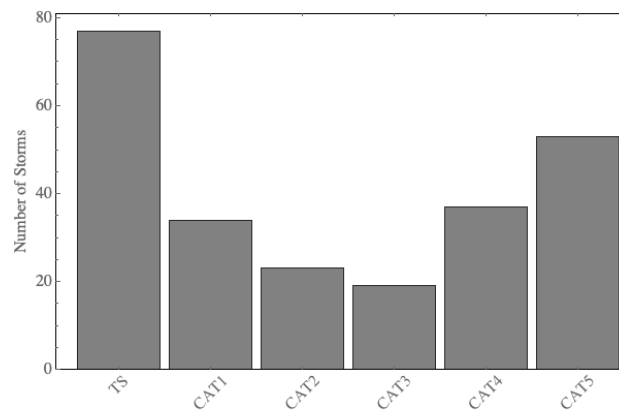


Figure 9. Divisions of the storm strengths after downscaling the results from the hurricane model. Abbreviations in figure are as follows: TS—Tropical storm, CAT1—Category 1, CAT2—Category 2, CAT3—Category 3, CAT4—Category 4, CAT5—Category 5.

The number of synthetic storms that fall into Tropical Storm to Category 3 strengths follows what has been historically seen within the North Carolina area [73]. The influence of climate change and the RCP 8.5 scenario can be seen in the significant number of storms that are classified as Category 4 and 5 strengths. Historically, the North Carolina coast has seen only a couple storms of Category 4 magnitude [64,73], one of which was Hurricane Hazel in 1954. Some of the more damaging storms in NC, such as Floyd, Fran, and Matthew, were Category 3 or lower at landfall, with the large damage due to associated rain and/or high surge from its more intense wind speed while offshore.

After the reduction of the number of storms, we also determined that the tracks developed from the hurricane model needed to be shortened due to the domain size of the hydrodynamic model, i.e., the ADCIRC domain extends to the 60th Meridian in longitude and some synthetic tracks extended beyond this. For model stability, it was necessary to remove the beginning portion of the tracks so that the resulting wind files started within the ADCIRC domain (this did not reduce the effects of the storms at landfall but only ensured that the storms would run within the coupled model system). To trim the spatial track extents, we utilized the following criteria: (1) all storms needed to start west of the 67th Meridian; and (2) loops in the storm track that remain within the ADCIRC domain were allowed. Additionally, because each of the synthetic storms was associated with a different year, it would require individual hydrodynamic spin-ups, a computational burden that would have minimal effect on total water levels. Thus, we removed this temporal information and assumed that each storm started at 0 UTC on September 6. After these reductions, all storm tracks were 4 to 5 days in duration.

4.2. Determining the P-CLIPER Frequency Coefficient

As part of the development of the precursor to the STORM-CoRe system, we examined the influence of the frequency parameter within the P-CLIPER model [18]. Results showed that there was a significant influence from this parameter in regard to precipitation rates and the resulting inundation levels within the Tar and Neuse River basins of North Carolina. Geoghegan et al. [34] evaluated historical storms within the North Carolina area and indicated that the frequency parameter, f -value, could range from -19 to 50 for these basins, but lower strength storms (Category 1 and 2) showed a tighter range of -18 to 38 . To account for this, we randomly sampled the f -value in P-CLIPER for the synthetic storms from the following ranges: Tropical Storms: -20 to 50 , Category 1 and 2 storms: -20 to 35 and Category 3, 4 and 5 storms: -20 to 35 .

The P-CLIPER model only computes precipitation when the synthetic storm track passes within 350 km of the model domain [34]. Additionally, P-CLIPER, in its current configuration, assumes a single storm strength throughout the simulation; therefore, the model in its current configuration assigns the largest storm strength found within the 350 km radius to the entire simulation. For example, a storm may start as a Category 2 storm near the edge of the 350 km P-CLIPER box but reduce to

a Tropical Storm nearer to the coast of North Carolina. In this case we would utilize the Category 2 storm throughout the P-CLIPER evaluation. Figure 10 shows the division of the strengths for the 243 storms as they are evaluated within the P-CLIPER domain. As can be seen when comparing Figures 9 and 10, there is a reduction in the strengths utilized in P-CLIPER relative to the largest recorded hurricane intensity, as storms typically reduce in intensity as they approach the coast. Based on these bin assignments for storm strength, we utilized random sampling of the appropriate *f*-value range (given above) to develop the associated rainfall for each storm using P-CLIPER.

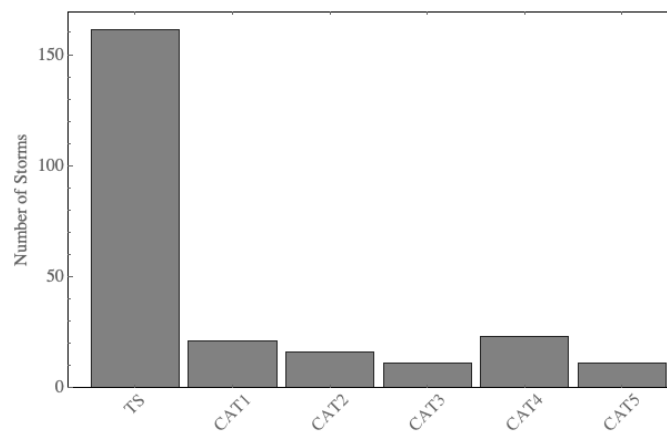


Figure 10. Division of the storm strengths that were evaluated by P-CLIPER within the 350 km radius of the North Carolina area. Abbreviations in figure are as follows: TS—Tropical storm, CAT1—Category I, CAT2—Category 2, CAT3—Category 3, CAT4—Category 4, CAT5—Category 5.

4.3. Determining ADCIRC Sea Level Rise

Many hurricane studies that utilize synthetic storms, e.g., coastal protection system studies [6,74,75], incorporate a set value for the sea level rise (SLR), say 0.33 to 1 m. In addition, they incorporate this sea level rise condition for the most severe storms or a select set of storms that encompass the range of the storm strengths (i.e., TS—Category 5). Herein, we wanted to incorporate uncertainty in sea level rise in a manner similar to what was used by the hurricane model itself and the frequency term in the P-CLIPER model. Therefore, we chose to follow the methodology utilized within the North Carolina area [76–78]. Since the synthetic hurricanes developed from the hurricane model discussed in Section 2.1 span years 2080 to 2100, we used the sea level rise for this same period. Table 2 shows the estimated sea level rise at five North Carolina tidal gauges during this time frame.

Next, a random sampling of SLR values was taken from this table for the years being evaluated. A beta distribution was used to determine the sampling and the following methodology was utilized: (1) the time-dependent mean value, upper bound and lower bound of sea level rise between the years of 2080–2100 were calculated using least square interpolation; (2) the sea level rise for each year was assumed to follow a beta distribution with the parameters, $q = r = 3$. One sample is generated for each hurricane event, such that there are 243 random samples in total. Figure 11a provides the random sampling of the sea level rise values for all events.

In order to limit the number of sea level rise scenarios being investigated due to computational considerations, we chose to combine the 243 points within the yearly beta distributions into 20 time-independent relative sea level rise bins by assigning each storm to the bin that was closest to its randomly sampled SLR value. The resulting bins are shown in Figure 11b and actual SLR values for each bin are given in Table 3.

Table 2. Relative sea level rise for three time periods considering potential rates of sea level rise from the RCP 8.5 study (RCP 8.5 which is the highest greenhouse gas emission scenario, combined with estimated vertical land movement at the tidal gauges).

RCP 8.5 Plus Vertical Land Movement					
Stations	Duck	Oregon Inlet	Beaufort	Wilmington	Southport
<i>Relative Sea Level Rise by 2080</i> (meters)					
Mean	0.55	0.51	0.51	0.47	0.48
Low	0.4	0.36	0.37	0.33	0.34
High	0.69	0.65	0.65	0.61	0.62
95% CI	0.14	0.15	0.14	0.14	0.14
<i>Relative Sea Level Rise by 2090</i> (meters)					
Mean	0.67	0.62	0.63	0.59	0.6
Low	0.5	0.45	0.46	0.42	0.43
High	0.84	0.8	0.8	0.76	0.77
95% CI	0.17	0.18	0.17	0.17	0.17
<i>Relative Sea Level Rise by 2100</i> (meters)					
Mean	0.81	0.75	0.76	0.71	0.72
Low	0.58	0.52	0.54	0.49	0.5
High	1.0	0.98	0.98	0.93	0.94
95% CI	0.22	0.23	0.22	0.22	0.22

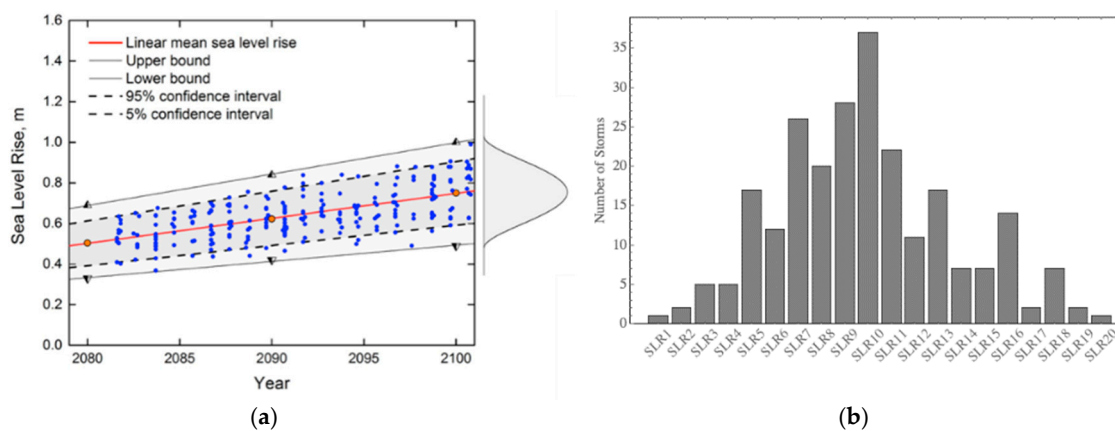


Figure 11. (a) Random samples of relative sea level rise for the 243 storms between the years 2080 to 2100, the blue dots represent each of the 243 storms and the grey region indicates the beta distribution between the lower and upper bounds; (b) final distribution of SLR scenarios after the 243 storms are combined into 20 bins to reduce computational requirements.

Table 3. Relative sea level rise values for the twenty scenarios used in this study.

Sea Level Rise (meters)				
SLR1: 0.3679	SLR2: 0.4053	SLR3: 0.4338	SLR4: 0.4721	SLR5: 0.4961
SLR6: 0.5231	SLR7: 0.5544	SLR8: 0.5861	SLR9: 0.6165	SLR10: 0.6450
SLR11: 0.6772	SLR12: 0.7012	SLR13: 0.7375	SLR14: 0.7643	SLR15: 0.7952
SLR16: 0.8262	SLR17: 0.8544	SLR18: 0.8791	SLR19: 0.9051	SLR20: 0.9898

4.4. Results from the STORM-CoRe System for the Synthetic Storms

Each of the 243 storms described in Section 4.1 was run with the STORM-CoRE system using the randomly sampled values for rain frequency (Section 4.2) and SLR (Section 4.3). For each storm, output from the ADCIRC model (time series and global maximums) were saved for water levels and velocities, wind speed and direction, and significant wave heights. These values were then passed on to the stochastic modeling team so that they could develop a statistical model that could be used for community resilience planning [26]. Additionally, the global results (water elevations, velocities, wind speed, and wave heights) are further combined into maximum of maximum files for each storm category (TS, CAT12, CAT345) and sea level rise scenario (SLR1 thru SLR20).

Below we illustrate the STORM-CoRe workflow with storm 4: Meteorological input from the hurricane and precipitation models is shown in Figure 12 and the resulting hydrologic and hydrodynamic output are shown in Figure 13; storm 4 is part of the SLR13 scenario and is a category4 storm at landfall with a randomly assigned rainfall frequency of 31. Additionally, a sample plot of maximum expected water elevations (combined storm surge and river runoff) within the resilience domain for all simulated CAT345 storms is shown in Figure 14.

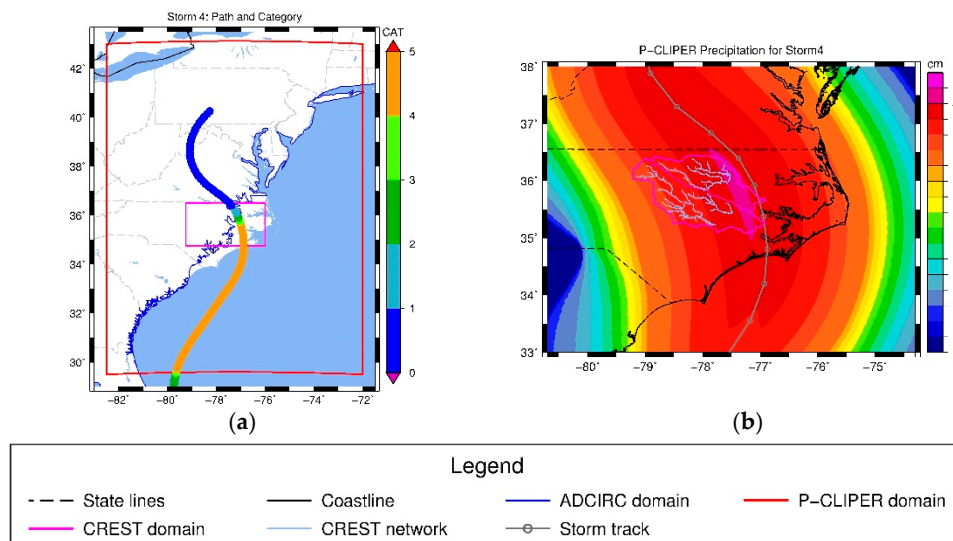


Figure 12. Meteorological input for Storm 4 in the stochastic STORM-CoRe process: (a) hourly synthetic hurricane track with storm strengths denoted by color scale (CAT4 at landfall and maximum within PCLIPER domain), (b) Accumulated precipitation (cm) near CREST model from P-CLIPER (CAT4 storm, $f = 0.31$).

Notice that the precipitation is higher over the Tar watershed, but that both watersheds range from 15–60 cm of total precipitation (Figure 12b). Additionally, all but Contentnea Creek have peak streamflows that occur after the rainfall has ended (indicated by short dashed line in Figure 13a). Significant windspeeds of 40–60 m/s go through the resilience zone and persist north of the study area (Figure 13b), while significant wave heights of 3–4 m extend up both the Tar and Neuse Rivers just to the CREST boundary (Figure 13c); total water level predicted by STORM-CoRe is shown in Figure 13d. Although not shown herein, comparison of the storm surge alone versus river runoff maximum elevation plots reveals that the maximum upland flooding in the both basins is due to the delayed river runoff (all contours upriver from the green band near -77.25 35.6 for the Tar River and all contours upriver from the slate band near -77.25 35.25 for the Neuse River in Figure 13d). Meanwhile, maximum flooding downriver from these points is due to the initial storm surge; none of the increased streamflow results in additional peaks in the coastal flooding. This is mirrored in the maximum envelope of water (MEOW) plot for all CAT345 storms shown in Figure 14, where the

maximum upland flooding is due to riverine flow while the maximum coastal flooding is due to initial storm surges.

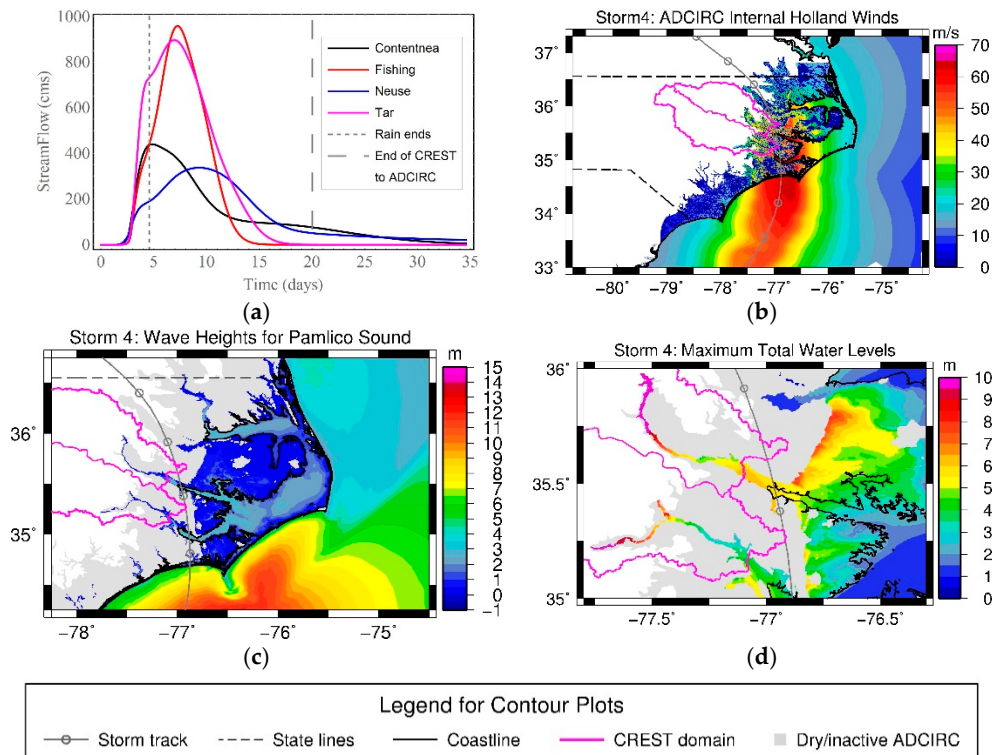


Figure 13. Hydrologic and hydrodynamic output for Storm 4 in the stochastic STORM-CoRe process: (a) hydrographs (cms) at four handoff points from CREST, (b) windspeed generated by Holland model within ADCIRC (m/s), (c) simulated wave height (m), and (d) maximum total water heights (m) relative to MSL, including storm surge and river runoff (6-h positions along storm track marked with dots).

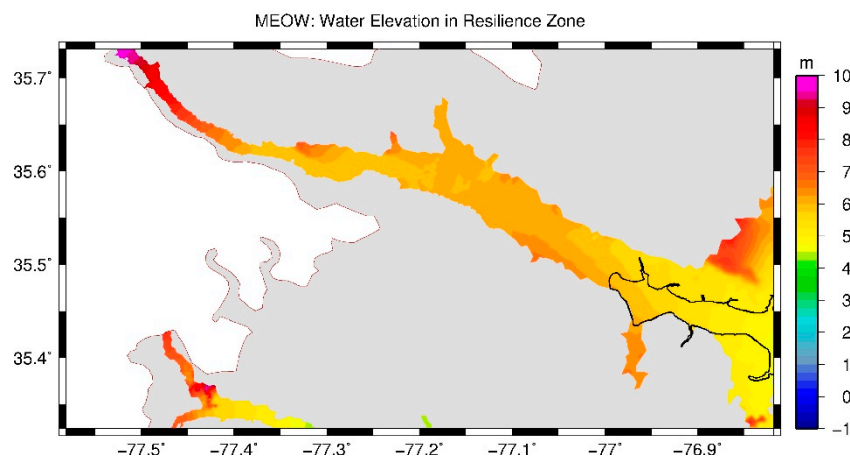


Figure 14. Maximum envelope of total water in the resilience area for all CAT345 storms; color bars indicate water level (m) relative to MSL, black line denotes coastline and gray region denotes the dry regions within the ADCIRC model.

5. Closing Remarks

A primary objective of this study was to develop and validate a coupled, physics-based, hydrologic/hydraulic system for modeling total water levels (rainfall, riverine flooding and storm surge) in response to tropical cyclones and hurricanes in coastal regions. Herein, we have defined the process, demonstrated the skill of the parametric models, and generated an ensemble of future scenarios based

on climate change projections. Example products, which are being used by the companion group for assessing community resilience [26], were also illustrated.

Author Contributions: Conceptualization, N.W., R.L.K. and K.M.D.; data curation, C.M.S., H.V. and K.M.D.; formal analysis, C.M.S. and K.M.D.; funding acquisition, N.W.; investigation, K.M.D., C.M.S., H.V., X.X. and J.X.; methodology, K.M.D., C.M.S., H.V., J.X. and X.X.; project administration, N.W. and R.L.K.; resources, N.W. and R.L.K.; software, K.M.D., C.M.S., H.V., K.M.G., J.X. and X.X.; supervision, R.K. and K.M.D.; validation, C.M.S., H.V. and K.M.D.; visualization, C.M.S.; writing—original draft, C.S. and K.D.; writing—review and editing, C.M.S., K.M.D. and R.L.K.

Funding: The research reported herein was supported by the Center for Risk-Based Community Resilience Planning as funded by the National Institute of Standards and Technology (NIST) under Cooperative Agreement No. 70NANB15H044, which is gratefully acknowledged.

Acknowledgments: Additional resources were provided by the University of Oklahoma, including computing resources by the OU Supercomputing Center for Education and Research (OSCER). ADCIRC visualizations were produced with FigureGen [79] and the Generic Mapping Toolkit (GMT [80]). Any opinions, conclusions, or findings are those of the authors and are not necessarily endorsed by the funding agencies.

Conflicts of Interest: The authors declare no conflict of interest. The funders had no role in the design of the study; in the collection, analyses, or interpretation of data; in the writing of the manuscript, or in the decision to publish the results.

References

1. Blake, E.S.; Zelinsky, D.A. *National Hurricane Center Tropical Cyclone Report Hurricane Harvey (AL092017) 17 August–1 September 2017*; Technical Report; National Oceanic and Atmospheric Administration National Hurricane Center: Miami, FL, USA, 2018.
2. Cangialosi, J.P.; Latta, A.S.; Berg, R. *National Hurricane Center Tropical Cyclone Report Hurricane Irma (AL112017) 30 August–12 September 2017*; Technical Report; National Oceanic and Atmospheric Administration National Hurricane Center: Miami, FL, USA, 2018.
3. Pasch, R.J.; Penny, A.B.; Berg, R. *National Hurricane Center Tropical Cyclone Report Hurricane Maria (AL152017) 16–30 September 2017*; Technical Report; National Oceanic and Atmospheric Administration National Hurricane Center: Miami, FL, USA, 2018.
4. NOAA's State of the Coast. *National Coastal Population Report: Population Trends from 1970 to 2020*; Technical Report; National Oceanic and Atmospheric Administration/United States Census Bureau: Washington, DC, USA, 2013.
5. International Panel on Climate Change (IPCC). *Climate Change 2014: Impacts, Adaptation, and Vulnerability: Part A: Global and Sectoral Aspects*; Contributions of Working Group II to the Fifth Assessment Report of the Intergovernmental Panel on Climate Change; Field, C., Ed.; Cambridge University Press: Cambridge, UK; New York, NY, USA, 2014; p. 1132.
6. Toro, G.R.; Resio, D.T.; Divoky, D.; Niedoroda, A.W.; Reed, C. Efficient joint-probability methods for hurricane surge frequency analysis. *Ocean Eng.* **2010**, *37*, 125–134. [[CrossRef](#)]
7. Yin, J.; Yu, D.; Lin, N.; Wilby, R.L. Evaluating the cascading impacts of sea level rise and coastal flooding on emergency response spatial accessibility in Lower Manhattan, New York City. *J. Hydrol.* **2017**, *555*, 648–658. [[CrossRef](#)]
8. Xian, S.; Yin, J.; Lin, N.; Oppenheimer, M. Influence of Risk Factors and Past Events on Flood Resilience in Coastal Resilience: Comparative Analysis of NYC and Shanghai. *Sci. Total Environ.* **2018**, *610–611*, 1251–1261. [[CrossRef](#)] [[PubMed](#)]
9. Hatzikyriakou, A.; Lin, N. Assessing the Vulnerability of Structures and Residential Communities to Storm Surge: An Analysis of Flood Impact during Hurricane Sandy. *Front. Built Environ.* **2018**, *4*, 1–13. [[CrossRef](#)]
10. Lin, N.; Shullman, E. Dealing with Hurricane Surge Flooding in a Changing Environment: Part 1. Risk Assessment Considering Storm Climatology Change, Sea Level Rise, and Coastal Development. *Stoch. Environ. Res. Risk Assess.* **2017**, *31*, 2379–2400. [[CrossRef](#)]
11. Lin, N.; Kopp, R.E.; Horton, B.P.; Donnelly, J.P. Hurricane Sandy's flood frequency increasing from year 1800 to 2100. *Proc. Natl. Acad. Sci. USA* **2016**, *113*, 12071–12075. [[CrossRef](#)]
12. Wahl, T.; Jain, S.; Bender, J.; Meyers, S.D.; Luther, M.E. Increasing risk of compound flooding from storm surge and rainfall for major US cities. *Nat. Clim. Chang.* **2015**, *5*, 1093–1097. [[CrossRef](#)]

13. Dresback, K.M.; Fleming, J.G.; Blanton, B.O.; Kaiser, C.; Gourley, J.J.; Tromble, E.M.; Luettich, R.A.; Kolar, R.L.; Hong, Y.; Van Cooten, S.; et al. Skill assessment of a real-time forecast system utilizing a coupled hydrologic and coastal hydrodynamic model during Hurricane Irene (2011). *Cont. Shelf Res.* **2013**, *71*, 78–94. [[CrossRef](#)]
14. Tromble, E.M.; Kolar, R.L.; Dresback, K.M.; Hong, Y.; Vieux, B.; Luettich, R.A.; Gourley, J.J.; Kelleher, K.E.; Van Cooten, S. Aspects of Coupled Hydrologic-Hydrodynamic Modeling for Coastal Flood Inundation. In Proceedings of the 11th International Conference on Estuarine and Coastal Modeling, Reston, VA, USA, 4–6 November 2009; Spaulding, M.L., Ed.; ASCE: Seattle, WA, USA, 2009; pp. 724–743.
15. Ray, T.; Stepinski, E.; Sebastian, A.; Bedient, P.B. Dynamic Modeling of Storm Surge and Inland Flooding in a Texas Coastal Floodplain. *J. Hydraul. Eng.* **2011**, *137*, 1103–1110. [[CrossRef](#)]
16. Torres, J.M.; Bass, B.; Irza, N.; Fang, Z.; Proft, J.; Dawson, C.; Kiani, M.; Bedient, P. Characterizing the hydraulic interactions of hurricane storm surge and rainfall–runoff for the Houston–Galveston region. *Coast. Eng.* **2015**, *106*, 7–19. [[CrossRef](#)]
17. Yang, K.; Davidson, R.; Vergara, H.; Kolar, R.L.; Dresback, K.M.; Colle, B.A.; Blanton, B.O.; Wachtendorf, T.; Trivedi, J.; Nozick, L.K. Incorporating Inland Flooding into Hurricane Evacuation Decision Support Modeling. *Nat. Hazards* **2019**, *96*, 857–878. [[CrossRef](#)]
18. Dresback, K.M.; Xue, X.; Xu, J.; Wang, N.; Kolar, R.L.; Geoghegan, K.M. STORM-CoRe: A Coupled Model System for Hurricanes, Storm Surge and Coastal Flooding to Support Community Resilience Planning under Climate Change. In Proceedings of the 12th International Conference on Structural Safety and Reliability, TU Wien, Vienna, Austria, 6–10 August 2017; p. 10.
19. Van Cooten, S.; Kelleher, K.E.; Howard, K.; Zhang, J.; Gourley, J.J.; Kain, J.S.; Nemunaitis-Monroe, K.; Flamig, Z.; Moser, H.; Arthur, A.; et al. The CI-FLOW Project: A System for Total Water Level Prediction from the Summit to the Sea. *Bull. Am. Meteorol. Soc.* **2011**, *92*, 1427–1442. [[CrossRef](#)]
20. Beven, J.; Cobb, H. *National Hurricane Center Tropical Cyclone Report Hurricane Isabel 6–19 September 2003*; Technical Report; National Oceanic and Atmospheric Administration National Hurricane Center: Miami, FL, USA, 2004.
21. Fleming, J.G.; Fulcher, C.W.; Luettich, R.A.; Estrade, B.D.; Allen, G.D.; Winer, H.S. A Real Time Storm Surge Forecasting System Using ADCIRC. In Proceedings of the 10th International Conference on Estuarine and Coastal Modeling, Reston, VA, USA, 5–7 November 2007; 2007; pp. 893–912.
22. Chu, P.; Blain, C.A.; Linzell, R.S. Development of a Relocatable Coastal Forecast System for the U.S. Navy. In Proceedings of the OCEANS 2009, MTS/IEEE Biloxi-Marine Technology for Our Future: Global and Local Challenges, Biloxi, MS, USA, 26–29 October 2009; pp. 1–8.
23. Flowerdew, J.; Horsburgh, K.; Wilson, C.; Mylne, K. Development and evaluation of an ensemble forecasting system for coastal storm surges. *Q. J. R. Meteorol. Soc.* **2010**, *136*, 1444–1456. [[CrossRef](#)]
24. Beardsley, R.C.; Chen, C.; Xu, Q. Coastal Flooding in Scituate (MA): A FVCOM Study of the 27 December 2010 Nor'easter. *J. Geophys. Res. Ocean.* **2013**, *188*, 6030–6045. [[CrossRef](#)]
25. Bowler, N.E.; Arribas, A.; Mylne, K.R.; Robertson, K.B.; Beare, S.E. The MOGREPS short-range ensemble prediction system. *Q. J. R. Meteorol. Soc.* **2008**, *134*, 703–722. [[CrossRef](#)]
26. Contento, A.; Xu, H.; Gardoni, P. Probabilistic Formulation for Climate Change Dependent Predictions of Storm Surge. *Struct. Infrastruct. Eng.* **2019**, in press.
27. Emanuel, K. Climate and Tropical Cyclone Activity: A New Model Downscaling Approach. *J. Clim.* **2006**, *19*, 4797–4802. [[CrossRef](#)]
28. Emanuel, K.; Ravela, S.; Vivant, E.; Risi, C. A Statistical Deterministic Approach to Hurricane Risk Assessment. *Bull. Am. Meteorol. Soc.* **2006**, *87*, 299–314. [[CrossRef](#)]
29. Emanuel, K.; Sundararajan, R.; Williams, J. Hurricanes and Global Warming: Results from Downscaling IPCC AR4 Simulations. *Bull. Am. Meteorol. Soc.* **2008**, *89*, 347–368. [[CrossRef](#)]
30. Oouchi, K.; Tomita, H.; Emanuel, K.; Satoh, M.; Yamada, Y. Comparison of Explicitly Simulated and Downscaled Tropical Cyclone Activity in a High-Resolution Global Climate Model. *J. Adv. Model. Earth Syst.* **2010**, *2*, 1–9. [[CrossRef](#)]
31. Russell, L.R. Probability Distributions for Texas Gulf Coast Hurricane Effects of Engineering Interest. Ph.D. Thesis, Stanford University, Palo Alto, CA, USA, 1968; p. 89.
32. Knutson, T.R.; McBride, J.L.; Chan, J.C.L.; Emanuel, K.; Holland, G.; Landsea, C.; Held, I.; Kossin, J.P.; Srivastava, A.K.; Sugi, M. Tropical cyclones and climate change. *Nat. Geosci.* **2010**, *3*, 157–163. [[CrossRef](#)]

33. O'Neill, B.C.; Oppenheimer, M.; Warren, R.; Hallegatte, S.; Kopp, R.E.; Pörtner, H.O.; Scholes, R.; Birkmann, J.; Foden, W.; Licker, R.; et al. IPCC reasons for concern regarding climate change risks. *Nat. Clim. Chang.* **2017**, *7*, 28–37. [[CrossRef](#)]
34. Geoghegan, K.M.; Fitzpatrick, P.; Kolar, R.L.; Dresback, K.M. Evaluation of a synthetic rainfall model, P-CLIPER, for use in coastal flood modeling. *Nat. Hazards* **2018**, *92*, 699–726. [[CrossRef](#)]
35. Wang, J.; Hong, Y.; Li, L.; Gourley, J.J.; Khan, S.I.; Yilmaz, K.K.; Adler, R.A.; Policelli, F.S.; Habib, S.; Irwin, D.; et al. The Coupled Routing and Excess Storage (CREST) Distributed Hydrological Model. *Hydrol. Sci. J.* **2011**, *56*, 84–98. [[CrossRef](#)]
36. Xue, X.; Hong, Y.; Limaye, A.S.; Gourley, J.J.; Huffman, G.J.; Khan, S.I.; Dorji, C.; Chen, S. Statistical and hydrological evaluation of TRMM-based Multi-satellite Precipitation Analysis over the Wangchu Basin of Bhutan: Are the latest satellite precipitation products 3B42V7 ready for use in ungauged basins? *J. Hydrol.* **2013**, *499*, 91–99. [[CrossRef](#)]
37. Burges, S.J.; Liang, X.; Lettenmaier, D.P.; Wood, E.F. A simple hydrologically based model of land surface water and energy fluxes for general circulation models. *J. Geophys. Res. Space Phys.* **1994**, *99*, 14415. [[CrossRef](#)]
38. Liang, X.; Wood, E.F.; Lettenmaier, D.P. Surface soil moisture parameterization of the VIC-2L model: Evaluation and modification. *Glob. Planet. Chang.* **1996**, *13*, 195–206. [[CrossRef](#)]
39. Ren-Jun, Z.; Yi-Lin, Z.; Le-Run, F.; Xin-Ren, L.; Quan-Sheng, Z. The Xinanjiang Model. *Hydrol. Forecast.* **1980**, *129*, 351–356.
40. Ren-Jun, Z. The Xinanjiang model applied in China. *J. Hydrol.* **1992**, *135*, 371–381. [[CrossRef](#)]
41. Gupta, V.; Duan, Q.; Sorooshian, S. Effective and efficient global optimization for conceptual rainfall-runoff models. *Water Resour. Res.* **1992**, *28*, 1015–1031. [[CrossRef](#)]
42. Duan, Q.Y.; Gupta, V.K.; Sorooshian, S.; Duan, Q. Shuffled complex evolution approach for effective and efficient global minimization. *J. Optim. Theory Appl.* **1993**, *76*, 501–521. [[CrossRef](#)]
43. Zhang, Y. Assimilation for Passive Microwave Streamflow Signals for Improving Flood Forecasting: A First Study in Cubango River Basin, Africa. *IEEE J. Sel. Top. Appl. Earth Obs. Remote Sens.* **2013**, *6*, 2375–2390. [[CrossRef](#)]
44. Clark, R.; Flamig, Z.; Vergara, H.; Hong, Y.; Gourley, J.; Mandl, D.; Frye, S.; Handy, M.; Patterson, M. Hydrological Modeling and Capacity Building in the Republic of Namibia. *Bull. Am. Meteorol. Soc.* **2016**, *98*, 1697–1715. [[CrossRef](#)]
45. Vergara, H.; Kirstetter, P.-E.; Gourley, J.J.; Flamig, Z.L.; Hong, Y.; Arthur, A.; Kolar, R.; Flamig, Z. Estimating a-priori kinematic wave model parameters based on regionalization for flash flood forecasting in the Conterminous United States. *J. Hydrol.* **2016**, *541*, 421–433. [[CrossRef](#)]
46. Gourley, J.J.; Flamig, Z.; Vergara, H.; Kirstetter, P.; Clark, R.; Argyle, E.; Arthur, A.; Martinaitis, S.; Terti, G.; Erlingis, J.; et al. The Flooded Locations and Simulated Hydrographs (FLASH) project: Improving the Tools for Flash Flood Monitoring and Prediction Across the United States. *Bull. Am. Meteorol. Soc.* **2017**, *98*, 361–372. [[CrossRef](#)]
47. Booij, N.; Ris, R.C.; Holthuijsen, L.H. A Third-Generation Wave Model for Coastal Regions, Part I: Model Description and Validation. *J. Geophys. Res.* **1999**, *104*, 7649–7666. [[CrossRef](#)]
48. Zijlema, M. Computation of wind-wave spectra in coastal waters with SWAN on unstructured grids. *Coast. Eng.* **2010**, *57*, 267–277. [[CrossRef](#)]
49. Dietrich, J.; Zijlema, M.; Westerink, J.; Holthuijsen, L.; Dawson, C.; Luettich, R.; Jensen, R.; Smith, J.; Stelling, G.; Stone, G. Modeling hurricane waves and storm surge using integrally-coupled, scalable computations. *Coast. Eng.* **2011**, *58*, 45–65. [[CrossRef](#)]
50. Luettich, R.A.; Westerink, J.; Scheffner, N. *ADCIRC: An Advanced Three-Dimensional Circulation Model for Shelves, Coasts and Estuaries, Report 1: Theory and Methodology of ADCIRC-2DDI and ADCIRC-3DL*; Technical Report DRP-92-6; Dredging Research Program; Department of the Army, U.S. Army Corp of Engineers, Waterways Experiment Station: Vicksburg, MS, USA; p. 1992.
51. U.S. Army Corp of Engineers (USACE). *ADCIRC and STWAVE Hydraulic Modeling of Southwest Coastal Louisiana Hurricane Protection Projects*; U.S. Army Corp of Engineers: New Orleans, LA, USA, 2011; p. 55.
52. Federal Emergency Management Agency (FEMA). *Flood Insurance Study: Coastal Counties, Texas, Intermediate Submission 2: Offshore Water Levels and Waves*; FEMA Region 6: Denton, TX, USA, 2011; p. 2903.
53. Blain, C.A.; Cambazoglu, M.K.; Linzell, R.S.; Dresback, K.M.; Kolar, R.L. The Predictability of Near-Coastal Currents Using a Baroclinic Unstructured Grid Model. *J. Ocean Dyn.* **2012**, *62*, 411–437. [[CrossRef](#)]

54. Bunya, S.; Dietrich, J.C.; Westerink, J.J.; Ebersole, B.A.; Smith, J.M.; Atkinson, J.H.; Jensen, R.; Resio, D.T.; Luettich, R.A.; Dawson, C.; et al. A High-Resolution Coupled Riverine Flow, Tide, Wind, Wind Wave, and Storm Surge Model for Southern Louisiana and Mississippi. Part I: Model Development and Validation. *Mon. Weather. Rev.* **2010**, *138*, 345–377. [[CrossRef](#)]
55. Dietrich, J.C.; Bunya, S.; Westerink, J.J.; Ebersole, B.A.; Smith, J.M.; Atkinson, J.H.; Jensen, R.; Resio, J.T.; Luettich, R.A.; Dawson, C.; et al. A High-Resolution Coupled Riverine Flow, Tide, Wind, Wind Wave, and Storm Surge Model for Southern Louisiana and Mississippi. Part II: Synoptic Description and Analysis of Hurricanes Katrina and Rita. *Mon. Weather Rev.* **2010**, *138*, 378–404. [[CrossRef](#)]
56. Blanton, B.; Dresback, K.; Colle, B.; Kolar, R.; Vergara, H.; Hong, Y.; Leonardo, N.; Davidson, R.; Nozick, L.; Wachtendorf, T. An Integrated Scenario Ensemble-Based Framework for Hurricane Evacuation Modeling: Part 2-Hazard Modeling. *Risk Anal.* **2018**. [[CrossRef](#)] [[PubMed](#)]
57. Szpilka, C.; Dresback, K.; Kolar, R.; Feyen, J.; Wang, J. Improvements for the Western North Atlantic, Caribbean and Gulf of Mexico ADCIRC Tidal Database (EC2015). *J. Mar. Sci. Eng.* **2016**, *4*, 72. [[CrossRef](#)]
58. Westerink, J.J.; Luettich, R.A., Jr.; Muccino, J.C. Modelling tides in the western North Atlantic using unstructured graded grids. *Tellus A Dyn. Meteorol. Oceanogr.* **1994**, *46A*, 178–199. [[CrossRef](#)]
59. Davidson, R.A.; Nozick, L.K.; Wachtendorf, T.; Blanton, B.; Colle, B.; Kolar, R.L.; Deyoung, S.; Dresback, K.M.; Yi, W.; Yang, K.; et al. An Integrated Scenario Ensemble-Based Framework for Hurricane Evacuation Modeling: Part 1-Decision Support System. *Risk Anal.* **2018**. [[CrossRef](#)]
60. Kinnmark, I. The Shallow Water Wave Equations: Formulation, Analysis and Application. *Lect. Notes Eng.* **1986**, *15*, 1–87.
61. Holland, G.J. An Analytic Model of the Wind and Pressure Profiles in Hurricanes. *Mon. Weather. Rev.* **1980**, *108*, 1212–1218. [[CrossRef](#)]
62. Gochis, D.J.; Barlage, M.; Dugger, A.; FitzGerald, K.; Karsten, L.; McAllister, M.; McCreight, J.; Mills, J.; RefieeiNasab, A.; Read, L.; et al. *The WRF-Hydro Modeling System Technical Description (Version 5.0)*; NCAR Technical Note; National Center for Atmospheric Research: Boulder, CO, USA, 2018; p. 107.
63. Massey, T.C.; Anderson, M.E.; Smith, J.M.; Gomez, J.; Jones, R. *STWAVE: Steady-State Spectral Wave Model User's Manual for STWAVE, Version 6.0*; ERDC/CHL SR-11-1; USACE Engineer Research and Development Center; Coastal and Hydraulics Laboratory: Vicksburg, MS, USA, 2011; p. 89.
64. Calvert, S.; Riva, M.; Rust, M. The Worst Hurricanes to Hit the Carolinas. *The Wall Street Journal*, 12 September 2018.
65. Cox, A.T.; Greenwood, A.J.; Cardone, V.J.; Swail, V.R. An Interactive Objective Kinematic Analysis System. In Proceedings of the Fourth International Workshop on Wave Hindcasting and Forecasting, Banff, AB, Canada, 16–20 October 1995; pp. 109–118.
66. Cardone, V.J.; Cox, A.T. Tropical Cyclone Wind Field Forcing for Surge Models: Critical Issues and Sensitivities. *Nat. Hazards* **2007**, *51*, 29–47. [[CrossRef](#)]
67. Powell, M.D.; Houston, S.H.; Amat, L.R.; Morisseau-Leroy, N. The HRD real-time hurricane wind analysis system. *J. Wind. Eng. Ind. Aerodyn.* **1998**, *77*, 53–64. [[CrossRef](#)]
68. URS. *Watershed Concepts, Task Order 272, Hurricane Isabel Rapid Response Coastal High Water Mark (CHWM) Collection*; FEMA Report 1490-DR-NC; Federal Emergency Management Agency: Washington, DC, USA, 2003.
69. NOAA National Data Buoy Center. Available online: <https://www.ndbc.noaa.gov/> (accessed on 1 February 2019).
70. NOAA Tides and Currents. Available online: <http://tidesandcurrents.noaa.gov> (accessed on 1 February 2019).
71. Emanuel, K. Massachusetts Institute of Technology. Personal Communication, August 2016.
72. McKay, M.D.; Beckman, R.J.; Conover, W.J. A Comparison of Three Methods for Selecting Values of Input Variables in the Analysis of Output from a Computer Code. *Technometrics* **1979**, *21*, 239. [[CrossRef](#)]
73. Landsea, C.W.; Franklin, J.L. Atlantic Hurricane Database Uncertainty and Presentation of a New Database Format. *Mon. Weather. Rev.* **2013**, *141*, 3576–3592. [[CrossRef](#)]
74. Wamsley, T.V.; Cialone, M.A.; Smith, J.M.; Ebersole, B.A.; Grzegorzewski, A.S. Influence of landscape restoration and degradation on storm surge and waves in southern Louisiana. *Nat. Hazards* **2009**, *51*, 207–224. [[CrossRef](#)]
75. United States Army Corp of Engineer (USACE). *Incorporating Sea Level Change in Civil Works Programs*; ER 1100-2-8162; U.S. Army Corp of Engineer: Washington, DC, USA, 31 December 2013.

76. N.C. Coastal Resources Commission Science Panel. *North Carolina Sea Level Rise Assessment Report*; Technical Report; N.C. Department of Environment and Natural Resources/Division of Coastal Management: Raleigh, NC, USA, 2010.
77. N.C. Coastal Resources Commission Science Panel. *Addendum to the North Carolina Sea Level Assessment Report of 2010*; Technical Report; N.C. Department of Environment and Natural Resources: Raleigh, NC, USA, 2012.
78. N.C. Coastal Resources Commission Science Panel. *North Carolina Sea Level Rise Assessment Report 2015*; Technical Report; N.C. Department of Environment and Natural Resources: Raleigh, NC, USA, 2015.
79. Dietrich, J.C.; Dawson, C.N.; Proft, J.M.; Howard, M.T.; Wells, G.; Fleming, J.G.; Luettich, R.A.; Westerink, J.J.; et al. Real-Time Forecasting and Visualization of Hurricane Waves and StormSurge Using SWAN+ADCIRC and FigureGen. In *Computational Challenges in the Geosciences, The IMA Volumes in Mathematics and Its Applications*; Springer: New York, NY, USA, 2013; Volume 156, pp. 49–70.
80. Wessel, P.; Smith, W.H.F.; Scharroo, R.; Luis, J.F.; Wobbe, F. Generic Mapping Tools: Improved version released. *EOS Trans. AGU* **2013**, *94*, 409–410. [[CrossRef](#)]



© 2019 by the authors. Licensee MDPI, Basel, Switzerland. This article is an open access article distributed under the terms and conditions of the Creative Commons Attribution (CC BY) license (<http://creativecommons.org/licenses/by/4.0/>).